Oncology and Translational Medicine
DOI 10.1007/s10330-020-0404-4

June 2020, Vol. 6, No. 3, P93–P97

ORIGINAL ARTICLE

Application of biological optimization of hypofractionated radiotherapy post conservative surgery for breast cancer*

Ying Shao [1, 2], Yadi Wang [1], Fuli Zhang [1] (✉), Shi Wang [3]

[1] Department of Radiotherapy, The Seventh Medical Center, PLA General Hospital, Beijing 100700, China
[2] Department of Radiotherapy, Beijing Tsinghua Changgung Hospital affiliated to Tsinghua University, Beijing 102218, China
[3] Department of Engineering Physics, Tsinghua University, Beijing 100084, China

Abstract

Objective The aim of the study was to discuss the application of biological optimization and its difference from physical optimization in hypofractionated radiotherapy for breast cancer after conservative surgery.
Methods This retrospective study enrolled 15 randomly chosen patients with left-sided breast cancer who received radiotherapy. The volumetric arc therapy (VMAT) technique was used to redesign treatment plans with physical functions (PF) group, biological-physical functions combined (BF + PF and PF + BF) groups, and biological functions (BF) group. The dosimetric differences based on the above four optimization methods were assessed by calculating and analyzing the corresponding dose-volume parameters.
Results The target parameters of the four groups differed significantly ($P < 0.05$) except for the conformity index (CI). The tumor control probability (TCP) values in the BF and BF + PF groups were higher than those in the PF and PF + BF groups. Moreover, the dose-volume parameters of the ipsilateral lung in the BF group were less than those of three other groups, while the monitor unit (MU) in the BF group was approximately 16% lower than those of the PF and PF + BF groups.
Conclusion Biological functions were useful to increase the equivalent uniform dose (EUD) and TCP values of the target, decrease the dose-volume parameters of the organs-at-risk (OARs), and improve treatment efficiency.

Received: 26 January 2020
Revised: 24 February 2020
Accepted: 6 March 2020

Key words: equivalent uniform dose (EUD); breast cancer; hypofractionated radiotherapy; dosimetry

In routine radiotherapy work, medical physicists achieve accurate dose calculations utilizing various treatment planning systems (TPS), which provide different types of optimization functions and algorithms to meet clinical dosimetry requirements. The physical function based on dose-volume parameters is simple and straightforward to use for the optimization of intensity-modulated radiotherapy (IMRT); however, its main disadvantage is that it does not reflect nonlinear responses of tumors and normal tissues to irradiation. By only utilizing a physical function to a certain point on the dose curve [1], the overall dose distribution of the target or organs-at-risk (OARs) cannot be adjusted; thus, it has certain limitations in constraining the overall dose to the tissue. The biological function based on the equivalent uniform dose (EUD) includes biological parameters reflecting the interaction between radiation and tissue, which can offset the limitations of the sole physical function optimization. Research and reports on breast cancer hypofractionation radiotherapy have confirmed that this treatment mode can achieve an equivalent effect to that for conventional fractionation, reducing the total cost to patients [2–6]. The present study evaluated the effects of different biological parameters on target EUD and tumor control probability (TCP) by comparing treatment plan optimization results based on physical functions (PF group), the combination of physical and biological functions (BF + PF and PF + BF groups), and

✉ Correspondence to: Fuli Zhang. Email: radiozfli@163.com
* Supported by a grant from the Beijing Municipal Science and Technology Commission (No. Z181100001718011).

biological functions (BF group), providing a dosimetric reference for clinical application.

Materials and methods

Patient data

Computed tomography (CT) scans from 15 patients with left-sided breast cancer (T1N0 carcinoma) treated at our hospital (The Seventh Medical Center, PLA General Hospital, Beijing, China) between July 2007 and January 2016 were analyzed. The median patient age was 55 (range: 33–63) years. The patients were placed in the supine position on a breast board (Med Tec, Orange City, IA) with both arms raised above their head and sternum parallel to the couch. Lead wires were placed to locate the breast, scar, and skin marks on the CT images. The patients were scanned from the level of the larynx to the level of the upper abdomen, including the left and right lungs, with 5-mm slice thickness and slice separations.

Target volumes

The delineation of target and critical structures for all patients was done by a single radiation oncologist with extensive experience in breast cancer treatment. The clinical target volumes (CTVs) included the breast defined as the glandular tissue apparent on CT scan, while the planning target volumes (PTVs) included the breast parenchyma with a 3-mm rim of the skin removed. Retraction of the breast contour 3-mm from the skin surface was used to account for dose build-up during dose calculation.

OARs

The OARs included the left and right lungs, the heart, and the contralateral breast. The esophagus, thyroid, and humeral head, though not mentioned in the following dose distribution analysis in this work, were also delineated.

Methods

The EUD is a concept of biological dose related to the biological characteristics of tissues proposed by Niemierko *et al* [7–8]. The EUD combines the physical dose with the TCP and normal tissue complication probability (NTCP) [8]. The most common formula is as follows:

$$EUD = (\frac{1}{N}\sum_{i=1} D_i^a)^{\frac{1}{a}} \quad (1)$$

where N is the number of voxels in the region of interest (ROI), D_i is the dose of the ith voxel in the ROI, and a is a biological parameter describing the dose-volume effect of the tumor or normal tissue. For tumors, a is usually a negative value with a larger absolute value; for serial OARs, a is usually a positive value with a larger absolute value; for parallel OARs, a is usually a positive value with a smaller absolute value [9–10]. In this study, to clearly show the relationship between the a value and the dose responses of the targets and normal lung tissues, the a value of the targets ranged from –100 to –10 with intervals of 10; for normal lung tissues, the a value ranged from 0.1 to 1.0 with intervals of 0.1 [11].

The TCP model is a logical model proposed by Bentzen *et al* [12], as follows:

$$TCP = \frac{1}{1+(\frac{TCD_{50}}{EUD})^{4\gamma_{50}}} \quad (2)$$

where TCD_{50} is the dose required when the tumor control rate reaches 50% and γ_{50} is the slope of the tumor tissue dose-response curve. TCD_{50} and γ_{50} are both obtained from large quantities of clinical data.

The NTCP model is based on the assumption that there is no volume effect between voxels of normal tissues [10] and has a formula similar to that for TCP:

$$NTCP = \frac{1}{1+(\frac{TD_{50}}{EUD})^{4\gamma_{50}}} \quad (3)$$

where TD_{50} is the dose required when the NTCP reaches 50% and γ_{50} is the slope of the dose-response curve of normal tissue and can be taken as $\frac{1}{m\sqrt{2\pi}}$, where m is a parameter related to the slope of the dose-response curve obtained from clinical data [12].

Designing treatment plans

CT images of 15 patients with left breast cancer receiving radiation therapy were chosen and volumetric arc modulation (VMAT) plans were redesigned on a Monaco 5.11 TPS (ElektaAB, Stockholm, Sweden). For each case, four plans were redesigned. First, both the target and the OARs were constrained by physical functions (PF group); second, the target was constrained by physical functions while the OARs were constrained by biological functions (PF + BF group); third, the target was constrained by biological functions while the OARs were constrained by physical functions (BF + PF group); fourth, both the target and OARs were constrained by biological functions (BF group). The prescription was set to 42.9 Gy/13 f [13], with at least 95% of the target volume surrounded by the prescribed dose. Two partial arcs of 200° were used with a starting angle of 150° an interval angle of 20° and a calculation uncertainty of 1%. When the four groups of plans were optimized, the same constraint parameters were selected.

Calculations and statistical analysis

Based on the dose-volume histogram (DVH) data derived from the treatment plan, MATLAB (version

2015a, MathWorks, US) was used to calculate: (1) the EUD and TCP values of the targets for each group for *a* values from –100 to –10 at intervals of 10; (2) the NTCP values of normal lung tissues for *a* values from 0.1 to 1.0 at intervals of 0.1. In addition, the homogeneity index (HI) and the conformity index (CI) of the target were also calculated and compared.

The calculation formula for HI was:

$$HI = \frac{D_{2\%} - D_{98\%}}{D_{50\%}} \times 100\% \quad (4)$$

in which $D_{2\%}$ approximately represents the maximum dose in the target, $D_{98\%}$ represents the minimum dose in the target, and $D_{50\%}$ is the median dose of the target.

The calculation formula for CI was:

$$CI = \frac{V_{T,Pi}}{V_T} \times \frac{V_{T,Pi}}{V_{Pi}} \quad (5)$$

where $V_{T,Pi}$ represents the target volume surrounded by the prescription dose, V_T represents the target volume, and V_{Pi} represents the total volume surrounded by the prescription dose [14].

One-way analysis of variance (ANOVA) was performed using IBM SPSS Statistics for Windows version 20.0 to analyze differences among groups; least significant difference (LSD) tests were used to analyze the differences between any two groups. Differences were considered statistically significant for $P < 0.05$.

Results

Target

The target indices are listed in Table 1. Except for CI, the differences among HI, MU, and beam-on time were statistically significant ($P < 0.05$). In addition, further LSD tests showed that the HIs of the target in the BF and the BF + PF groups were slightly worse than those in the other two groups (both $P < 0.05$); while the MU was significantly reduced, that in the BF group was reduced by about 16% compared to those in the PF and PF + BF groups (both $P < 0.05$). Therefore, the two groups of plans using biological functions had higher delivery efficiency.

Table 2 lists the EUD values of the targets of the four groups with the value of *a* ranging from –100 to –10. Only when *a* was set to –10 were significant differences observed among the four groups ($P < 0.05$). Further LSD tests showed that the EUD of the BF group was slightly higher than those of PF and PF + BF groups (both $P < 0.05$).

We also calculated and analyzed the target TCP of the four groups. Fig. 1 shows the relationship between the value of *a* and the target TCP.

OARs

Fig. 2 shows the transverse isodose distributions of the four planning groups in a single patient. The dose gradient of the BF group was larger than those of other three groups; the dose line is more compact and the ipsilateral lung received a smaller dose.

Fig. 3 shows a DVH diagram of the four groups of plans for a single patient. The DVH curve of the PTV in the BF group was significantly shifted to the right, while

Table 1 Indices of the target for the four groups of plans ($\bar{\chi} \pm s$)

Index	PF group	PF + BF group	BF group	BF + PF group	*P* value	*F* value
HI	0.097 ± 0.010	0.095 ± 0.009	0.113 ± 0.013	0.111 ± 0.009	0.000	11.610
CI	0.829 ± 0.031	0.828 ± 0.025	0.852 ± 0.028	0.843 ± 0.025	0.061	2.603
MU	1209.63 ± 111.77	1200.39 ± 166.03	1006.75 ± 57.22	1069.84 ± 105.54	0.000	10.952
BeamOn (min)	3.37 ± 0.37	3.37 ± 0.35	2.96 ± 0.32	3.09 ± 0.30	0.002	5.769

Table 2 EUD of the target ($\bar{\chi} \pm s$)

a value	PF group (Gy)	PF + BF group (Gy)	BF group (Gy)	BF + PF group (Gy)	*P* value	*F* value
–100	45.48 ± 6.76	45.33 ± 6.41	45.79 ± 7.20	45.28 ± 6.99	0.997	17.299
–90	45.95 ± 6.73	45.80 ± 6.37	46.27 ± 7.18	45.77 ± 6.98	0.997	0.405
–80	46.54 ± 6.69	46.37 ± 6.31	46.86 ± 7.16	46.36 ± 6.96	0.997	0.097
–70	47.27 ± 6.63	47.09 ± 6.21	47.60 ± 7.12	47.11 ± 6.92	0.997	0.041
–60	48.18 ± 6.51	48.02 ± 6.07	48.56 ± 7.06	48.09 ± 6.85	0.996	0.026
–50	49.30 ± 6.28	49.19 ± 5.82	49.80 ± 6.93	49.38 ± 6.72	0.994	0.020
–40	50.61 ± 5.84	50.62 ± 5.38	51.26 ± 6.57	51.02 ± 6.45	0.989	0.018
–30	51.97 ± 5.01	52.06 ± 4.57	52.76 ± 5.71	52.70 ± 5.70	0.961	0.017
–20	53.21 ± 3.43	53.27 ± 2.99	54.35 ± 3.95	54.19 ± 4.08	0.750	0.017
–10	54.31 ± 0.62	54.26 ± 0.54	55.72 ± 0.82	55.50 ± 0.85	0.000	0.017

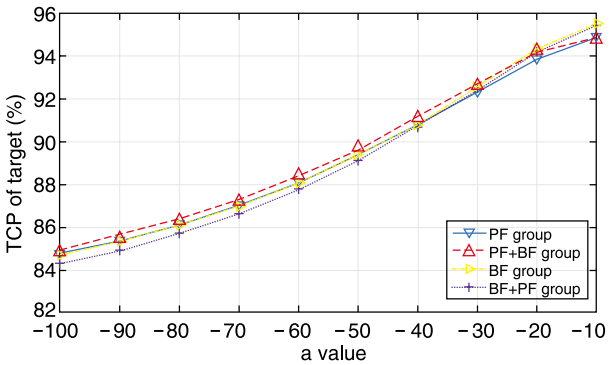

Fig. 1 Relationship between TCP and *a* value of the target

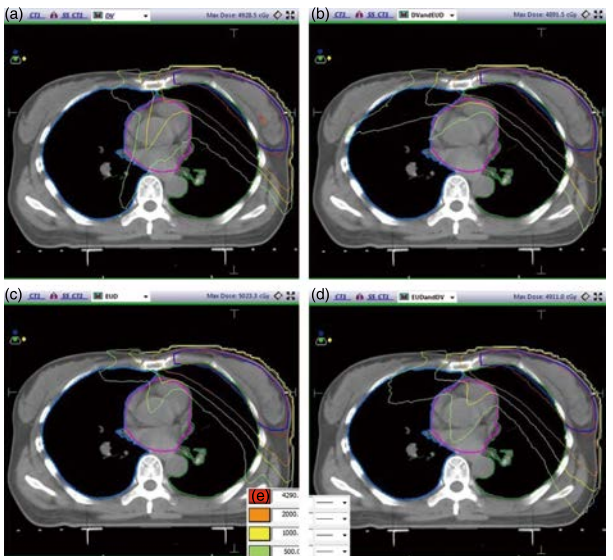

Fig. 2 Transverse isodose distributions of the four groups of plans in a single patient. (a–d) Dose distributions in the PF, PF + BF, BF and BF + PF groups, respectively; (e) Color sketch of the isodose line

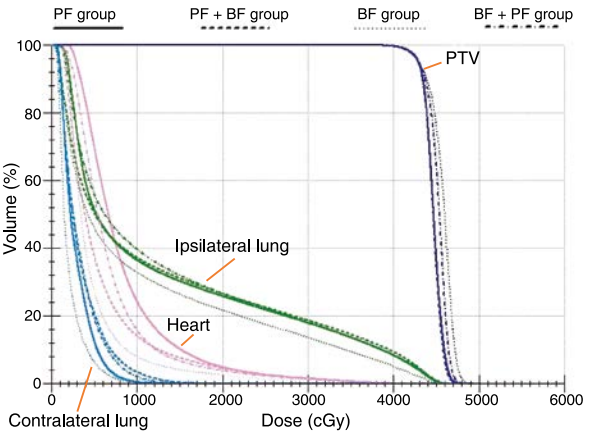

Fig. 3 DVH of the four groups for a specific patient

the DVH curves of the bilateral lung and heart were significantly shifted to the left.

Table 3 shows the dose-volume parameters of the lung and heart obtained using the four optimization methods. The irradiated dose of the ipsilateral lung and heart in the EUD group is lower than those of the other three groups. Significant differences in the ipsilateral lung V_5, V_{10}, and V_{30}; D_{mean}; and heart V_{20} were observed among the four groups ($P < 0.05$). LSD tests demonstrated a lower ipsilateral lung V_5 in the BF group compared to those in the other three groups ($P < 0.05$ for all). The ipsilateral lung V_{10} and D_{mean} in the BF group were lower than those of the PF and PF + BF groups (all $P < 0.05$). The ipsilateral lung V_{20} and V_{30} in the BF group were lower than those of the PF + BF group (all $P < 0.05$). The heart V_{20} in the BF group was lower than those of the PF and PF + BF groups (all $P < 0.05$).

Table 3 Dose-volume parameters of the organs-at-risk ($\bar{\chi} \pm s$)

Parameter	PF group	PF + BF group	BF group	BF + PF group	*P* value	*F* value
Ipsilateral lung V_5 (%)	68.19 ± 12.43	60.28 ± 6.51	52.67 ± 7.36	63.41 ± 12.15	0.001	6.387
Ipsilateral lung V_{10} (%)	39.46 ± 5.64	39.69 ± 3.95	35.19 ± 4.65	37.83 ± 4.69	0.046	2.844
Ipsilateral lung V_{20} (%)	26.21 ± 4.15	27.40 ± 3.67	24.11 ± 3.72	24.72 ± 4.32	0.111	2.096
Ipsilateral lung V_{30} (%)	19.13 ± 3.52	20.61 ± 3.16	17.21 ± 2.96	17.57 ± 3.79	0.030	3.217
Ipsilateral lung D_{mean} (Gy)	12.06 ± 1.54	12.17 ± 1.36	10.62 ± 1.40	11.34 ± 1.70	0.023	3.427
Contralateral lung V_5 (%)	24.98 ± 12.03	25.10 ± 11.52	24.21 ± 12.15	24.96 ± 9.08	0.996	0.020
Contralateral lung V_{10} (%)	5.37 ± 4.44	5.25 ± 4.26	5.15 ± 4.72	6.26 ± 4.44	0.898	0.197
Contralateral lung D_{mean} (Gy)	3.15 ± 0.81	3.14 ± 0.82	3.03 ± 0.85	3.15 ± 0.67	0.968	0.085
Heart V_{10} (%)	34.70 ± 14.19	35.25 ± 14.55	30.63 ± 12.12	27.34 ± 12.44	0.333	1.160
Heart V_{20} (%)	14.72 ± 7.37	13.55 ± 6.62	30.63 ± 12.12	27.34 ± 12.44	0.000	11.345
Heart V_{30} (%)	7.15 ± 4.86	6.19 ± 3.86	5.03 ± 3.73	6.19 ± 4.84	0.617	0.601
Heart D_{mean} (Gy)	8.72 ± 2.40	8.46 ± 2.22	7.77 ± 1.87	7.58 ± 2.24	0.433	0.929
Cord D_{max} (Gy)	4.41 ± 1.51	3.40 ± 1.75	3.61 ± 2.35	3.70 ± 1.95	0.504	0.791
Contralateral breast V_5 (%)	10.16 ± 8.95	12.43 ± 6.66	11.41 ± 7.06	11.09 ± 8.90	0.890	0.209
Contralateral breast D_{max} (Gy)	6.67 ± 0.81	7.46 ± 1.18	6.95 ± 1.03	6.22 ± 0.68	0.006	4.543
Contralateral breast D_{mean} (Gy)	2.59 ± 0.51	2.69 ± 0.48	2.67 ± 0.46	2.68 ± 0.48	0.935	0.141

Discussion

In our study, optimization based on the biological function increased the D_{mean} of the target. The D_{max} of the target was also increased, which further reduced the uniformity of the target. No significant differences in target CI were observed among the four groups. The biological function was more sensitive to the cold spot in calculating the dose of the target but was not sensitive enough to the hot spot. Therefore, it was not possible to control the hot spot more effectively while increasing the cold spot dose, which increased the D_{max} and D_{mean} and reduced the uniformity of the target. In addition, the MU in the BF group was significantly lower than those of the PF and PF + BF groups, which significantly improved the efficiency of treatment delivery. This advantage is more applicable to clinical work in most radiotherapy departments in China [15].

For OARs, biological function significantly reduced the exposure dose to the ipsilateral lung, showing its absolute advantage in protecting normal lung, while physical function reduced the D_{max} of the contralateral breast. In addition, the relationships between the various dose-volume parameters of the heart, LAD, and spinal cord and biological and physical functions were not obvious. One explanation may be the presence of a dynamic dose balance in the dose distribution. When the dose of the ipsilateral lung was limited, the dose curve would be shifted to the adjacent normal tissues such as the heart or contralateral lung. Second, the spinal cord was away from the target and most of the exposure came from scattering. Therefore, the differences among the four groups were not enough to demonstrate the advantages of biological and physical functions. In addition, LAD had strong individual variability, with the differences in LAD irradiated dose among the four groups greatly affected by its relative anatomical position to the target.

In short, biological function showed a clear advantage in increasing the target dose and decreasing the ipsilateral lung dose and played a positive role in improving TCP and reducing NTCP. The hypofractionation radiotherapy model is becoming increasingly prevalent and the role of biological optimization cannot be ignored. However, this study had several limitations. The relevant biological parameters used in the study were obtained from extensive early clinical experience that requires renewal to further the potential advantages of biological functions in planning.

Conflicts of interest

The authors indicated no potential conflicts of interest.

References

1. Senthilkumar K, Maria Das KJ, Balasubramanian K, *et al*. Estimation of the effects of normal tissue sparing using equivalent uniform dose-based optimization. J Med Phys, 2016, 41: 123–128.
2. Janssen S, Glanzmann C, Lang S, *et al*. Hypofractionated radiotherapy for breast cancer acceleration of the START a treatment regime: intermediate tolerance and efficacy. Radiat Oncol, 2014, 9: 165.
3. Haviland JS, Mannino M, Griffin C, *et al*. Late normal tissue effects in the arm and shoulder following lymphatic radiotherapy: Results from the UK START (Standardisation of Breast Radiotherapy) trials. Radiother Oncol, 2018, 126: 155–162.
4. Chatterjee S, Arunsingh M, Agrawal S, *et al*. Outcomes following a moderately hypofractionated adjuvant radiation (START B type) schedule for breast cancer in an unscreened non-Caucasian population. Clin Oncol (R Coll Radiol), 2016, 28: e165–e172.
5. START Trialists' Group, Bentzen SM, Agrawal RK, *et al*. The UK Standardisation of Breast Radiotherapy (START) trials B of radiotherapy hypofractionation for treatment of early breast cancer: a randomised trial. Lancet, 2008, 371: 1098–1107.
6. Haviland JS, Owen JR, Dewar JA, *et al*. The UK Standardisation of Breast Radiotherapy (START) trials of radiotherapy hypofractionation for treatment of early breast cancer: 10-year follow-up results of two randomised controlled trials. Lancet Oncol, 2013, 14: 1086–1094.
7. Niemierko A. Reporting and analyzing dose distributions: A concept of equivalent uniform dose. Med Phys, 1997, 24: 103–110.
8. Thieke C, Bortfeld T, Niemierko A, *et al*. From physical dose constraints to equivalent uniform dose constraints in inverse radiotherapy planning. Med Phys, 2003, 30: 2332–2339.
9. Wu QW, Mohan R, Niemierko A, *et al*. Optimization of intensity-modulated radiotherapy plans based on the equivalent uniform dose. Int J Radiat Oncol Biol Phys, 2002, 52: 224–235.
10. Hu HQ, Zhang HW, Qiu XP. Optimization results of biological equivalent uniform dose in intensity modulated radiotherapy. Chin J Med Physics, 2016, 33: 190–194.
11. Wang C, Gu JL, Deng QH, *et al*. Clinical value of lung equivalent uniform dose in predicting VMAT-induced radiation pneumonitis. Chin J Radiat Oncol (Chinese), 2017, 26: 749–753.
12. Bentzen SM, Tucker SL. Quantifying the position and steepness of radiation dose-response curves. Int J Radiat Biol, 1997, 71: 531–542.
13. Yarnold J, Ashton A, Bliss J, *et al*. Fractionation sensitivity and dose response of late adverse effects in the breast after radiotherapy for early breast cancer: long-term results of a randomised trial. Radiother Oncol, 2005, 75: 9–17.
14. International Commission on Radiation Units and Measurements. Report 83: prescribing, recording and reporting photon-beam intensity-modulated radiation therapy (IMRT). J ICRU, 2010, 10: 1–106.
15. Lang JY, Wang P, Wu DK, *et al*. An investigation of the basic situation of radiotherapy in the mainland of China in 2015. Chin J Radiat Oncol (Chinese), 2016, 25: 541–545.

DOI 10.1007/s10330-020-0404-4
Cite this article as: Shao Y, Wang YD, Zhang FL, *et al*. Application of biological optimization of hypofractionated radiotherapy post conservative surgery for breast cancer. Oncol Transl Med, 2020, 6: 93–97.